FEBS Letters 351 (1994) 437–442

FEBS 14523

The crystal structure of the iron-free cytochrome *c* peroxidase and its implication for the enzymatic mechanism

Xiao-Dong Su[a], Takashi Yonetani[b], Ulf Skoglund[a,*]

[a]*Department of Cell and Molecular Biology, Medical Nobel Institute, Karolinska Institutet, S-171 77 Stockholm, Sweden*
[b]*Department of Biochemistry and Biophysics, School of Medicine, University of Pennsylvania, Philadelphia, PA 19104-6089, USA*

Received 18 July 1994; revised version received 1 August 1994

Abstract We report the refined structure of an iron-free form of cytochrome *c* peroxidase (CcP) at 2.3 Å resolution. The backbone comparison between native CcP and iron-free CcP shows that the two structures have the same protein fold within experimental error. The only difference noted is in the heme pocket where the distance between the proximal histidine and the center of the protoporphyrin has increased. The results show that the iron-free CcP should be a good substitute for native CcP in fluorescence studies and thus also validate previous studies using iron-free CcPs as efficient fluorescent probes in electron transfer studies.

Key words: Cytochrome *c* peroxidase; Protoporphyrin IX; Heme; X-ray crystallography; Electron transfer; Cytochrome *c*

1. Introduction

Cytochrome *c* Peroxidase (CcP, ferrocytochrome *c*:H_2O_2 oxidoreductase, EC 1.11.1.5) is a monomeric, heme-containing enzyme that consists of 294 residues. Found exclusively in aerobically grown yeast, it catalyzes the peroxide-dependent oxidation of cytochrome *c* (cyt *c* or *cc*) in the following multistep reaction:

$$CcP_{(Fe^{3+})} + H_2O_2 \rightarrow CcP_{(Fe^{4+}=O^{2-})}* + H_2O \quad (1)$$

$$CcP_{(Fe^{4+}=O^{2-})}* + \text{cyt } c_{(Fe^{2+})} + H^+ \rightarrow CcP_{(Fe^{4+}=O^{2-})} + \text{cyt } c_{(Fe^{3+})} \quad (2)$$

$$CcP_{(Fe^{4+}=O^{2-})} + \text{cyt } c_{(Fe^{2+})} + H^+ \rightarrow CcP_{(Fe^{3+})} + \text{cyt } c_{(Fe^{3+})} + H_2O \quad (3)$$

H_2O_2 oxidizes ferric CcP to $CcP_{(Fe^{4+}=O^{2-})}*$, so-called compound I, which consists of a ferryl (Fe^{4+}) iron and a semistable amino acid-centred free radical denoted by the asterisk in the above scheme. The radical has been characterized as Trp^{191} [1]. Compound I is reduced back to the resting state in two consecutive one-electron transfer steps using two cytochrome *c* molecules as the reducing substrate.

The crystal structures of CcP [2], compound I [3,4], and the complexes between yeast CcP and cytochrome *c* from yeast and horse heart [5] have provided insights into how CcP is oxidized by H_2O_2, and how it interacts with cytochrome *c* to form an electron transfer complex. Recently, kinetics studies by the Laue method [4] have shown that there is little change in the overall structure during the reaction, except in the vicinity of the iron center.

In the present study, the effect of iron binding on the protein environment was investigated by solving the crystal structure of iron-free CcP. Iron-free CcP can be made by combining apoCcP with porphyrins such as protoporphyrin IX or mesoporphyrin IX [6]. Iron-free CcPs have been used as probes in the complex formed between horse heart cytochrome *c* and iron-free CcP when studied with the fluorescence quenching technique [7] and electric field effects by high-resolution fluorescence spectroscopy [8]. The refined iron-free CcP structure is presented here at 2.3 Å resolution, illuminating some of the functions of the ferric iron in the active site of the CcP molecule.

2. Materials and methods

Native CcP was isolated from baker's yeast and purified as previously described with modifications [9,10]. The protein was split into heme and apoprotein by acid 2-butanone [11,12]. Iron-free CcP was prepared by adding protoporphyrin IX in slight excess to apoCcP. The protoporphyrin IX apoCcP complex was purified by ion-exchange chromatography [6].

2-Methyl-2,4-pentanediol (MPD) was purchased from Fluka, and it was double vacuum distilled prior to use. All other crystallization reagents were purchased from Merck.

Structure analysis and refinement were primarily carried out with the program X-PLOR [13]. CCP4 package programs were used whenever necessary. Program O [14] was used for model building and to display and analyze the structures graphically.

2.1. Crystallization

All crystallization experiments were carried out at 4–7°C. Native CcP crystals were grown by the hanging or sitting drop vapor diffusion method with macro seeding. 4–7 μl of protein solution with a concentration about 15 mg/ml was applied to the drops for crystallization experiments. A roughly equal volume of the reservoir solution was added to the drops and after 1–2 days of equilibration, a tiny piece of CcP crystal was injected into the drop to induce crystal growth. The reservoir solution contained 30–35% MPD in 50 mM potassium phosphate buffer, pH 5.9. The crystallization trials were not successful until distilled MPD was used. The crystals belong to the space group $P2_12_12_1$ with unit cell parameters $a = 107.2$, $b = 77.2$, $c = 51.9$ Å, as reported previously [15].

Crystallization of iron-free CcP was similar to that of native CcP but proceeded in two steps. First, in order to get isomorphous crystals, iron-free CcP crystals were grown by cross-seeding with native CcP crystals. Then, the crystals were grown by seeding with iron-free CcP seeds. The hanging drop crystals were used for data collection because the sitting drop crystals appeared much flatter. The typical size of the prism-shaped crystals used for data collection was 0.5 mm × 0.5 mm × 0.3 mm. The crystals are isomorphous to the native CcP crystal within experimental error, with unit cell parameters $a = 107.8$, $b = 76.7$, $c = 51.7$ Å [16,17]. The unit cell of the native CcP was used for data procession and refinement.

*Corresponding author. Fax: (46) (8) 313529.

SSDI 0014-5793(94)00910-4

2.2. Data collection and processing

Diffraction data were collected from single crystals of both native and iron-free CcP using a Xentronics area detector system mounted on a Rigaku 200 rotating anode X-ray source operating at 40 kV, 70–90 mA. The diffraction angle offset of the detector was 20 degrees and the crystal to detector distance 11.0 cm. The data collection was performed at 20°C. The frame size was typically 0.1667 degrees with a sweep around the omega-axis of 90–120 degrees. The data sets were collected by a 0.3-mm collimator with an exposure time of 100–150 s.

Both the native and iron-free data sets were initially reduced using the on-line XENGEN package of programs. Subsequently the program XDS [18] was found to improved quality on the density maps. Therefore, XDS was used for processing the iron-free data sets. Table 1 shows the statistics of the data sets used for this work.

2.3. Structure analysis and refinement

The published CcP [2] structure was obtained from the Brookhaven protein data bank (PDB) [19,20] with the code 2CYP and used as the starting model for all subsequent refinements. The PDB CcP was refined by X-PLOR using the original structure factors obtained from the data bank (since the PDB CcP was not refined by X-PLOR) in order to enable a comparison between the PDB CcP structure and our native CcP structure.

The simulated annealing (SA) refinement was performed in the absence of water at 3,000K for both native and iron-free CcP. Then, water was added to the structures using the original PDB coordinates. SA refinements were performed again, followed by an individual B-factor refinement. Water molecules with B-factors greater than 60.0 were deleted from the structures. At this stage, the 2fo-fc and fo-fc maps were checked and the structure was remodelled when necessary. Finally, a full refinement (including SA refinement at 1,500K, free-R check, B-factor refinement and a geometry analysis) was carried out for both native and iron-free CcP. For PDB CcP, only the full refinement was performed at 1,500K. The results of the refinement are shown in Table 2.

3. Results and discussion

Previous studies have demonstrated that heme can be removed from native CcP and a porphyrin inserted into the apoCcP under nearly denaturing conditions [11,12] and that erroneously folded CcP molecules can be correctly refolded after interaction with cytochrome *c* [21]. Apparently the CcP molecule has the potential to attain different conformations. Thus it was not obvious that the structure of iron-free CcP would be the same as that of the native CcP. Here we report the structure of an iron-free form of CcP, i.e. apoCcP protoporphyrin IX complex, refined at 2.3 Å resolution.

The iron-free CcP crystal is isomorphous with native CcP and the statistics of Tables 1 and 2 show that iron-free CcP data are very similar to the native CcP data. The R-factors of iron-free CcP were lower than those of PDB CcP, while the free-Rs are higher as shown in Table 2. This may be explained by the fact that the iron-free CcP data are less complete than PDB CcP data.

Fig. 1 shows that the two structures have the same protein fold within experimental error in spite of the lack of iron. Similar findings have been reported for ribonucleotide reductase, a non-heme diferric protein [22].

In Fig. 2, a portion of 2fo-fc map of iron-free CcP is shown around the active site. In addition to the well solved protein structure, there is a cluster of water molecules at the distal side of the protoporphyrin IX. Compared with the native CcP, the water molecules are a bit more shifted to the side of the protoporphyrin IX. The differences in water distribution in the active site might indicate a natural variability, since it has been shown that the ferric ion in native CcP is either penta- or hexa-coordinated [28]. The sixth ligand is a water molecule. There is also evidence that the native CcP with a hexa-coordinated iron is a more stable and less active form of the enzyme [29]. Obviously the native CcP has some flexibility in the active site, shown by the different positions and hydrogen bonding of its water molecules. This flexibility could facilitate a rapid access to the active site for the polar hydrogen peroxide substrate.

Some side-chain atoms are not visible in both native and iron-free CcP maps. Most of the missing atoms from the 25 residues in the published native CcP [2] are still not visible in our maps. However, some of them, (e.g. Leu^{4} CG1 and Val^{10} CG2), can be seen in the iron-free CcP maps.

In Fig. 3, the nicely resolved protoporphyrin IX structure compares well with the corresponding heme in the native structure as well as its position within the protein molecule. To our knowledge, this is the first time a protoporphyrin IX structure has been determined in a protein. The heme and protoporphyrin IX structures display great similarity except at the iron center. Both protoporphyrin IX and heme are a bit skewed. This skewness must emanate from the interaction of the protoporphyrin IX with the apoprotein molecule, or be an expression of intrinsic properties of the protoporphyrin IX. Therefore, the influence of the iron can be regarded as negligible in this respect. The skewness has been noted also in spectroscopic measurements on mesoporphyrin IX CcP [8].

A difference Fourier between the native CcP and iron-free CcP shows no significant peaks except at the active site where a strong iron peak can be noted (Fig. 4). The red positive density in the center highlights the missing iron, which has been reported to be 0.2 Å below the heme plane [2]. In accordance with this, the major volume of the red density is below the plane of the protoporphyrin IX. The blue negative density is mostly around the nitrogen atoms that were formerly the iron ligands. There is also a minute density in the water cluster site (see arrow in Fig. 2). The perturbations in the vicinity of the protoporphyrin IX include mainly a 0.5-Å shift of the distal residue His^{175} away from the putative iron site. The reported distance between His^{175} and the iron in heme is 1.95 Å [2], but our data indicate that this distance is increased to 2.47 Å in the iron-free form.

Compared with PDB CcP the proximal His^{175} is 0.5 Å further away from the 'would-be-site' of the iron ion in iron-free CcP (Fig. 4), without being accompanied by main chain shift. The His^{175} displacement can be explained by the removed charge supplied by the iron ion in native CcP. It also has 20–30% higher B-factors compared with the corresponding values in

Table 1
Data collection statistics

Protein crystals	Merged data sets	Resolution cutoff (Å)	Unique reflections	Completeness (%)	R_{merge}[a] (%)
Native CcP	1	2.3	17017	87.2	6.2
Iron-free CcP	2	2.3	15918	80.6	8.2

[a] $R_{merge} = \Sigma|I_{obs} - I_{avg}|\Sigma I_{obs}$ where the summation is over all reflections in the merged data set(s).

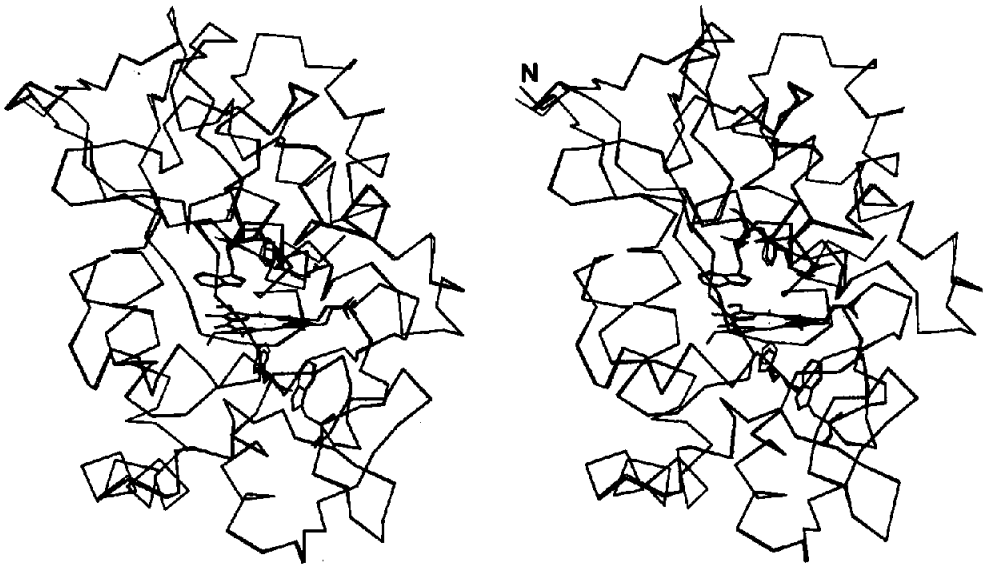

Fig. 1. Stereo drawing of C_α back bone comparison between the iron-free CcP (thick line) and the native CcP (thin line) with protoporphyrin IX, heme, and some active site residues superimposed. The RMS deviation of the C_α carbon 4–293 between these two structures is 0.159 Å. N-terminal is indicated by N.

native CcP after overall B-factor correction (but the protoporphyrin IX in iron-free CcP and the heme in native CcP have the same B-factors). This indicates that it is more flexible when not coordinated by the iron ion. It is then plausible to assume that the observed closer association of His^{175} to the iron ion in native CcP [2] merely reflects a more frequently used rotamer conformation for the His^{175}. Again, this indicates a de-emphasized role of the iron for the main chain folding in native CcP.

Several high resolution crystal structures of CcP have been obtained. But regardless if the enzyme is in the native state, in complex with carbon monoxide [23], nitric oxide [24], cyanide or fluoride [23,25], or in the peroxide-oxidized Compound I [3,4], or has a mutated residue close to the iron site [26,27], the CcP protein backbone fold displays a remarkably conserved structure in all cases. Even when the CcP has formed a complex with its electron donor substrate, cytochrome *c*, its structure

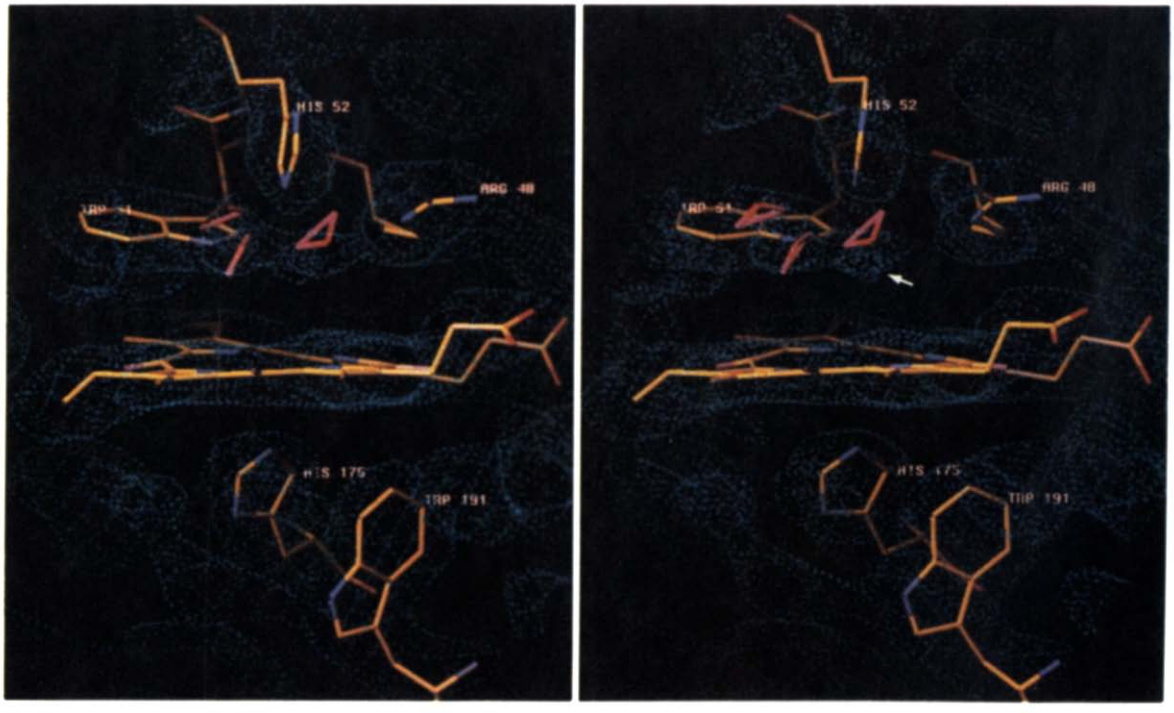

Fig. 2. Stereo pair of the 2fo-fc map of iron-free CcP showing the active site region. The refined iron-free CcP structure is shown as stick model with the residue names labelled. The map was calculated by using $(2|Fo|-|Fc|)\exp(i\alpha c)$ as Fourier coefficients, where Fo and Fc are the observed and calculated structure factors, respectively, and αc is the calculated phase from the final model. The electron density was contoured at average density 1.1 times the root mean square deviation of the map. The arrow indicates a density that corresponds to a cluster of 3 water molecules shown as triangles.

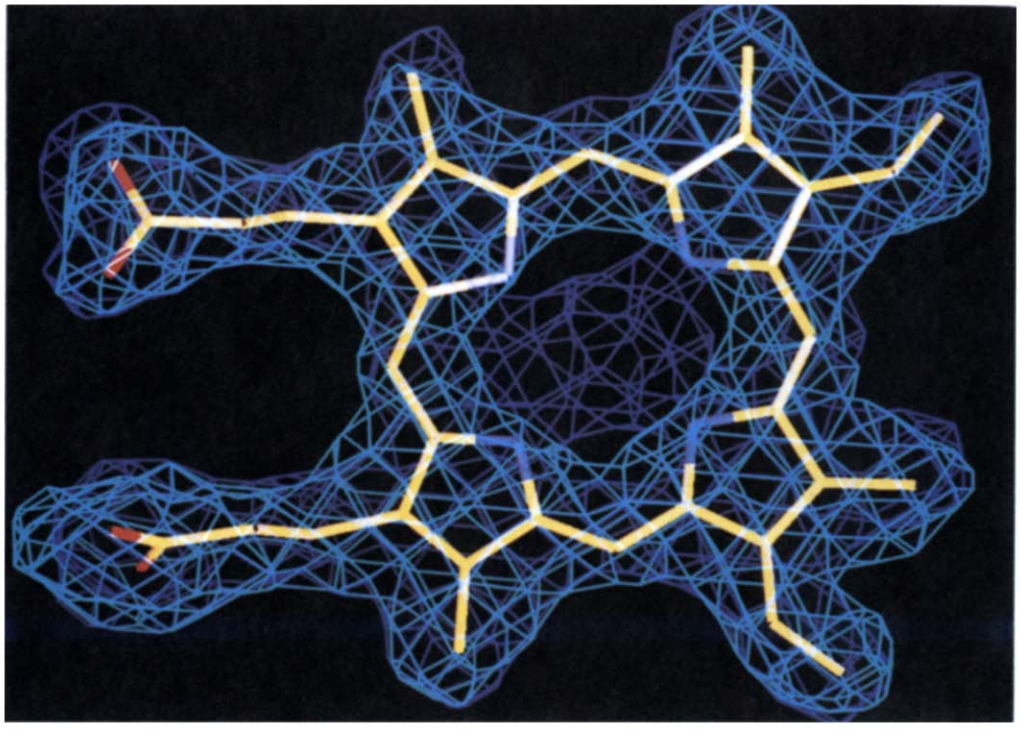

Fig. 3. 'Direct omit' maps of the protoporphyrin IX (cyan) and heme (blue) superimposed with the protoporphyrin IX model. The maps were made by omitting the correspondent residue (protoporphyrin IX for iron-free CcP, heme for native CcP) from the iron-free and native CcP structures. Then, fo-fc maps were calculated using (|Fo|−|Fc|)exp(iαc) as Fourier coefficients. Fo and Fc are the observed and calculated structure factors, respectively, and αc is the calculated phase from the final refined models. The electron density was contoured at average density +3.0 × the root mean square deviation of the map.

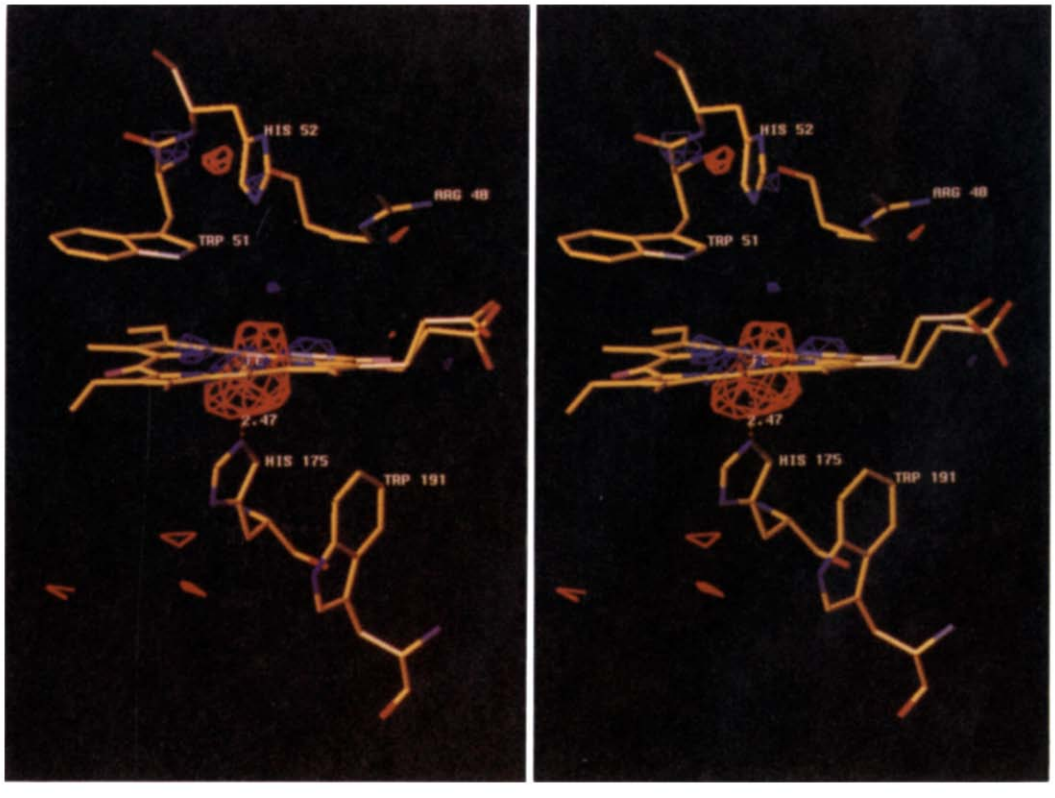

Fig. 4. The difference Fourier map around the iron centre. It was calculated by using $(|F_{native}|-|F_{iron\text{-}free}|)\exp(i\alpha c)$ as Fourier coefficients, where F_{native} and $F_{iron\text{-}free}$ are the native and iron-free CcP structure factors, respectively, and ac is the calculated phase from the refined iron-free CcP model. The density was contoured at average density ± 4.2 × the root mean square deviation of the map with positive density in red and negative in blue. The distance between the 'iron site' and His^{175} NE2 is 2.47 Å as indicated.

Table 2
X-plor refinement statistics

Name of the data sets	No. of reflections used	No. water molecules included	SA[a] refinement R	free-R	B-factor[b] refinement R	free-R	RMS[c] of bond (Å)	RMS[c] of angle (deg.)	RMS[d] of comparisons
Iron-free CcP	14,760	215	14.2	21.7	13.7	22.7	0.011	2.52	0.198
Native CcP	15,870	261	14.7	20.2	14.2	20.8	0.012	2.44	0.152
PDB CcP*	18,488	263	16.2	20.8	15.8	21.6	0.012	2.41	0.162

*The refined native CcP structure with the structure factors from PDB data bank.
[a] Simulated annealing refinement by X-PLOR.
[b] Individual B-factor refinement by X-PLOR.
[c] The root-mean-square deviations of the bond lengths and bond angles in the final structures from the ideal values.
[d] The root-mean-square deviations of the Cα carbon (between C4-C293) of the listed structure from the published one [2]. The values are calculated by program O.

compares well with the native conformation [5]. A common theme in all these structures is that the iron ion has a variable position along the axis orthogonal to the plane of the protoporphyrin IX, and that there are some water molecule rearrangements upon ligand binding and some small side chain shifts for amino acids close to the iron. Consequently, the function of the heme iron ion in native CcP could be described as non-structural for the protein folding, but with an important role as a supplier of the needed ligand field for its coordinated and thus polarized atoms.

In fluorescence quenching techniques the iron-free CcP has been used to probe the heme–heme distance in the complex formed with cytochrome *c* [7]. It has been argued that those experiments were less reliable due to the uncertainty of the structure of the probe. It was later shown [30] that at least the dissociation constant was the same for the complex formed between iron-free and native CcP [7]. The results presented here show unambiguously that the iron-free CcP is an appropriate substitute for native CcP in fluorescence studies.

The stability of the active site environment in native CcP, demonstrated by the similarity to its iron-free form, is further underlined by the fact that the known radical confinement site, Trp^{191} [1], can be substituted by glycine with almost no consequence for the folding of the protein [27]. The Gly^{191} mutated form of CcP can be brought to the state of Compound I. The Trp^{191} seems to be only the first place for harbouring of the radical. After continued oxidation, or ageing, the Trp^{191} can get back its electron by donors probably localized among some aromatic residues around the Trp^{191} [31].

Why does the CcP protein have such a stable structure? The small spatial rearrangements are used as arguments to explain the fast reaction mechanism for CcP [4]. One can also argue that the stable structure is needed if the CcP enzyme is prepared to accept reducing electrons in a promiscuous way. The CcP enzyme could be forming a complex [5], or it could even extract the electrons internally [31]. The studies on proton exchange rates in the interface region between CcP and cytochrome *c* show that the region is more accessible [32] than expected from the crystallographic structure [5], and that some structural rearrangement can occur in the complex [33]. The stable structure of the heme environment certainly renders the concept of multiple electron transfer pathways possible [10], and underlines again the distance in electron transfer as an important parameter [34]. It is clear that the iron-free CcP, because of its fluorescence properties and almost identical structure to native CcP, will be a very efficient probe to use in further studies of electron transfer pathways.

Acknowledgements: This work has been in part supported by NIH Grants (GM48130 and HL14508) (T.Y.), Kjell and Märta Beijers Stiftelse (U.S.), Petrus and Augusta Hedlunds Stiftelse (U.S.), Gertrud and Ivar Philipsons Stiftelse (U.S.), Karolinska Institutet (U.S.) and Swedish Research Council for Engineering Sciences (TFR) (U.S.). The authors thank professor Christopher Mathews for critical review of the manuscript.

References

[1] Sivaraja, M., Goodin, D.B., Smith, M. and Hoffman, B.M. (1989) Science 245, 738–740.
[2] Finzel, B.C., Poulos, T.L. and Kraut, J. (1984) J. Biol. Chem. 259, 13027–13036.
[3] Edwards, S.L., Nguyen, H.X., Hamlin, R.C. and Kraut, J. (1987) Biochemistry 26, 1503–1511.
[4] Fülöp, V., Phizackerley, R.P., Soltis, S.M., Clifton, I.J., Wakatsuki, S., Erman, J., Hajdu, J. and Edwards, S.L. (1994) Structure 2, 201–208.
[5] Pelletier, H. and Kraut, J. (1992) Science 258, 1748–1755.
[6] Asakura, T. and Yonetani, T. (1969) J. Biol. Chem. 244, 537–544.
[7] Leonard, J.J. and Yonetani, T. (1974) Biochemistry 13, 1465–1468.
[8] Anni, H., Vanderkooi, J.M., Sharp, K.A., Yonetani, T., Hopkins, S.C., Herenyi, L. and Fidy, J. (1994) Biochemistry 33, 3475–3486.
[9] Yonetani, T. and Ray, G.S. (1965) J. Biol. Chem. 240, 4503–4508.
[10] Bosshard, H.R., Anni, H. and Yonetani, T. (1991) in: Peroxidases in Chemistry and Biology (Everse, J., Everse, K.E. and Grisham, M.B. Eds.) pp. 51–84, CRC Press, Boca Raton, FL.
[11] Teale, F.W.J. (1959) Biochim. Biophys. Acta 35, 543–543.
[12] Yonetani, T. (1967) J. Biol. Chem. 242, 5008–5013.
[13] Brünger, T.A., Kuriyan, J. and Karplus, M. (1987) Science 235, 458–460.
[14] Jones, T.A., Zou, J.-Y., Cowan, S.W. and Kjeldgaard, M. (1991) Acta Crystallogr. A47, 110–119.
[15] Hagman, L., Larsson, L.O. and Kierkegaard, P. (1969) Int. J. Prot. Res. 1, 283–288.
[16] Larsson, L.O., Hagman, L., Kierkegaard, P. and Yonetani, T. (1970) J. Biol. Chem. 245, 902–903.
[17] Skoglund, U., Structure and Function of Cytochrome *c* Peroxidase, PhD thesis, University of Stockholm, 1979.
[18] Kabsch, W. (1988) J. Appl. Crystalogr. 21, 916–924.
[19] Bernstein, F.C., Koetzle, T.F., Williams, G.J.B., Meyer, J.E.F., Brice, M.D., Rodgers, J.R., Kennard, O., Shimanouchi, T. and Tasumi, M. (1977) J. Mol. Biol. 112, 535–542.
[20] Abola, E.E., Bernstein, F.C., Bryant, S.H., Koetzle, T.F. and Weng, J. (1987) in: Crystallographic Databases – Information Content, Software Systems, Scientific Applications (Allen, F.H., Bergerhoff, G. and Sievers, R. Eds.) pp. 107–132, Data Commission of the International Union of Crystallography, Bonn/Cambridge/Chester.
[21] Hake, R., McLendon, G. and Corin, A.F. (1990) Biochem. Biophys. Res. Commun. 172, 1157–1162.
[22] Åberg, A., Nordlund, P. and Eklund, H. (1993) Nature 361, 276–260.

[23] Edwards, S.L. and Poulos, T.L. (1990) J. Biol. Chem. 265, 2588–2595.
[24] Edwards, S.L., Kraut, J. and Poulos, T.L. (1988) Biochemistry 27, 8074–8081.
[25] Edwards, S.L., Poulos, T.L. and Kraut, J. (1984) J. Biol. Chem. 259, 12984–12988.
[26] Wang, J.M., Mauro, M., Edwards, S.L., Oatley, S.J., Fishel, L.A., Ashford, V.A., Xuong, N.H. and Kraut, J. (1990) Biochemistry 29, 7160–7173.
[27] Fitzgerald, M.M., Churchill, M.J., McRee, D.E. and Goodin, D.B. (1994) Biochemistry 33, 3807–3818.
[28] Yonetani, T. and Anni, H. (1987) J. Biol. Chem. 262, 9547–9554.
[29] Smith, M.L., Paul, J., Ohlsson, P.I., Hjortsberg, K. and Paul, K.G. (1991) Proc. Natl. Acad. Sci. USA 88, 882–886.
[30] Vitello, L.B. and Erman, J.E. (1987) Arch. Biochem. Biophys. 258, 621–629.
[31] Fox, T., Tsaprailis, G. and English, A.M. (1994) Biochemistry 33, 186–191.
[32] Jeng, M.-F., Englander, S.W., Pardue, K., Rogalskyj, J.S. and McLendon, G. (1994) Nature Struct. Biol. 1, 234–238.
[33] Hahm, S., Miller, M.A., Geren, L., Kraut, J., Durham, B. and Millett, F. (1994) Biochemistry 33, 1473–1480.
[34] Moser, C.C., Keske, J.M., Warncke, K., Farid, R.S. and Dutton, P.L. (1992) Nature 355, 796–802.